

# Study on Power Assist Control of Push Cart Robot with Wheel-Side Encoder

Wataru Akada\* Student Member, Hiroshi Fujimoto\* Member

Push cart robot is one of the robots which utilize the idea of backdrivability and is expected to be used in various industrial fields. The geared wheel units of the push cart robot used in the experiment are modeled by two inertia system, and they have wheel side encoders at the gear. This study focuses on building control mechanism to improve the usability of the push cart robot. It is preferred to be pushed with smaller force, and to prevent the load on it from slipping. Impedance control is applied to make the robot easier to be pushed with smaller force. However, it can result in letting the load on the robot slip, causing it to drop. To prevent this, we propose friction force observer to observe the friction force between the load and the robot. It detect the switch of static friction and kinetic friction to detect the slip of the load. Effectiveness of both impedance control and friction force observer is demonstrated by simulations and experiments.

**Keywords:** push cart robot, two inertia system, impedance control, friction force observer

## 1. Introduction

Recently, robots are working in various fields, such as industry, surgery, and nursing care<sup>(1)(2)</sup>. Robots, especially mobile robots, often make contacts with human each other<sup>(3)</sup>. Thus, there are many studies to improve backdrivability<sup>(4)</sup> to prevent danger occurred by the contacts<sup>(5)(6)</sup>.

Push cart robot is one of the robotic applications where high backdrivability is required. A push cart robot is expected to be used in various industries to carry loads<sup>(7)</sup>.

The purpose of this study is to improve the usability of the push cart robot in two ways. First, it is preferred to be pushed with smaller force. We discuss impedance control to achieve this goal. Second, it should prevent it's load from slipping and dropping. Friction observer is proposed to realize this.

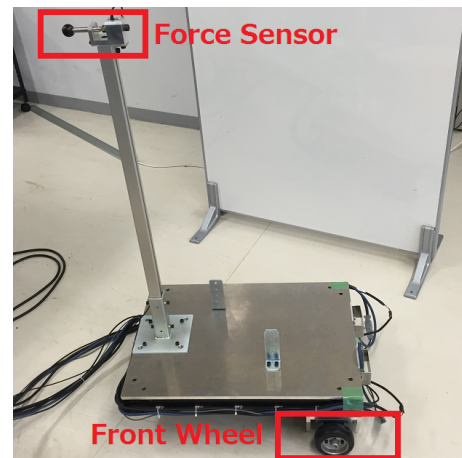
Characteristics and model of push cart robot used in experiments is presented in Section II. In Section III, power assist control using impedance control is proposed and it's effectiveness is demonstrated by simulation and experimental results. Section IV shows the model of push cart robot with load on it, and friction force observer is proposed to prevent the slip of the load, verified with simulations and experiment. Finally, the paper is concluded in Section V.

## 2. Push Cart Robot

In this section, the characteristics and model of push cart robot are explained. Mechanical parameters of the wheels are derived by parameter identification.

### 2.1 Characteristics and the model of the Push Cart Robot

Push cart robot used in this study is shown in Fig. 1. It is made to carry the load, by controlling the velocity of the



(a) Overall view



(b) Wheels

Fig. 1. Appearance of push cart robot

wheels. The push cart robot has two front wheels and one rear wheel. Front wheels are driving wheels which have motors to move the robot, while the rear wheel is non-driving wheel and is used to measure the velocity of cart body.

Front wheels with harmonic gears<sup>(9)</sup> are modeled by two-inertia system<sup>(8)</sup>. They have wheel-side encoders which were used to be difficult to mount due to limitation of space<sup>(10)</sup>. They also have torque sensors to measure torsion torque<sup>(11)</sup>.

\* The University of Tokyo  
5-1-5, Kashiwanoha, Kashiwa, Chiba 227-8561, Japan

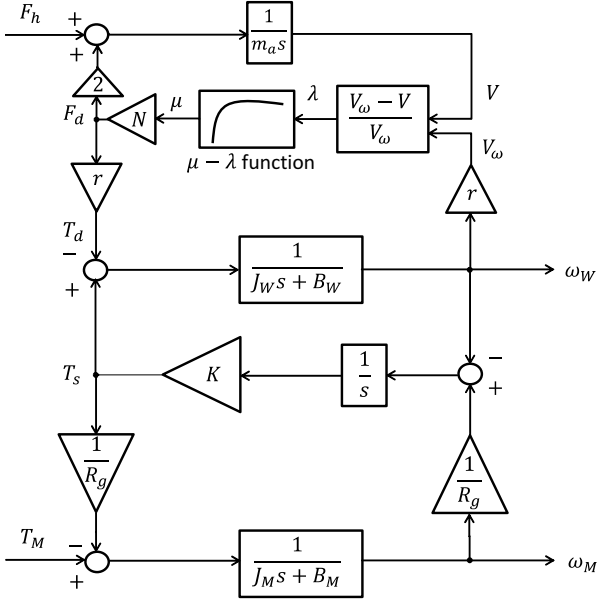


Fig. 2. Block diagram of the push cart robot

In the handle of the push cart robot, force sensor is included to measure external pushing force by the pusher. Block Diagram of this robot including slip factor is shown in Fig. 2.

## 2.2 Parameters of the Push Cart Robot

Physical parameters of the push cart robot are shown in Tab. 1. To identify the mechanical parameter of the wheels, parameter identification shown in Fig. 3 is executed. In this identification, chirp signal is put as the input of motor torque  $T_M$ . The frequency response from  $T_M$  to motor angular velocity  $\omega_M$  and wheel angular velocity  $\omega_W$  are measured. Identified mechanical parameters are shown in Tab. 2.

In Fig. 2,  $T_s$ ,  $T_d$  are torsion torque, driving torque,  $V_\omega$ ,  $V$  are rear wheel angular velocity, cart velocity, and  $F_h$ ,  $F_d$  are external pushing force and driving force.  $\mu$  and  $\lambda$  are friction coefficient and slip ratio of the wheel<sup>(12)</sup>, and have relation shown in Fig. 4, while braking is not considered.  $N$  is normal force exerted from each front wheels.

Table 1. Parameters of the push cart robot

| Parameter                    | Value   |
|------------------------------|---------|
| Wheel radius $r$             | 0.05 m  |
| Push cart mass $m_a$         | 30.6 kg |
| Reduction rate of gear $R_g$ | 31      |

Table 2. Identified parameters

| Parameter                              | Value  | Unit              |
|--|--------|-------------------|
| Motor side inertia $J_M$               | 5.5e-6 | kg·m <sup>2</sup> |
| Motor side viscosity coefficient $B_M$ | 5.0e-4 | N·m/(rad/s)       |
| Torque stiffness coefficient $K$       | 1950   | N·m/rad           |
| Wheel side inertia $J_W$               | 6.0e-4 | kg·m <sup>2</sup> |
| Wheel side viscosity coefficient $B_W$ | 8.5e-2 | N·m/(rad/s)       |

## 3. Impedance Control of the Push Cart Robot to Improve Backdrivability

Main goal of the push cart robot is to carry the load. It

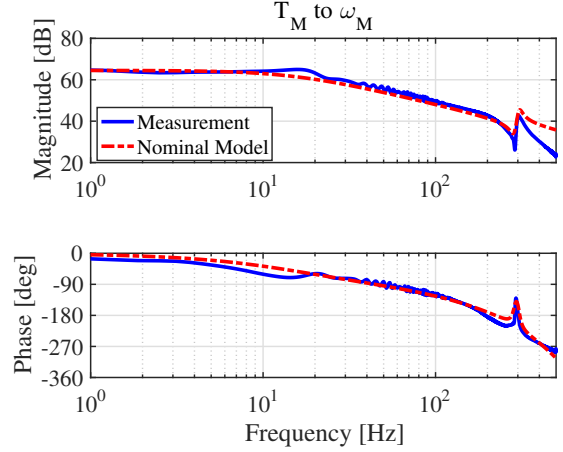
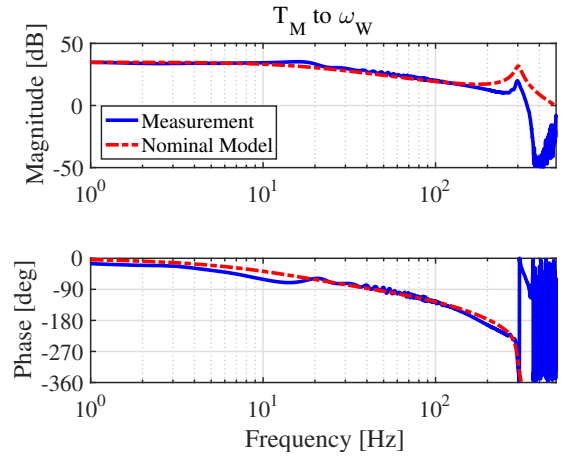

 (a)  $T_M$  to  $\omega_M$ 

 (b)  $T_M$  to  $\omega_W$ 

Fig. 3. Frequency responses

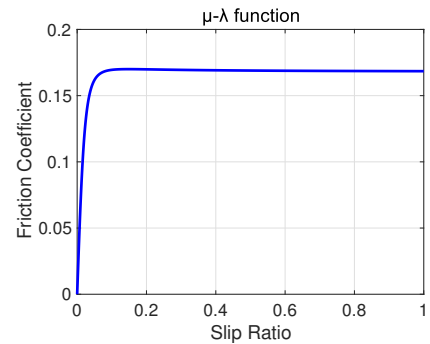


Fig. 4. Relation between slip ratio and friction coefficient of the wheel

is desired that the pusher do not feel it heavy, regardless the weight of the load. Impedance control is applied to enable push cart robot to move with smaller pushing force.

### 3.1 Overview of Impedance Control

Impedance control is a control method to adjust position and force of mechanical system by controlling mechanical

impedance such as mass and damper of the robot<sup>(13)</sup>. Here, we use velocity reference based on virtual mass  $M_i$  and virtual damper  $B_i$ , which is lighter than actual mass and damper, making it easier to push with smaller force. Block diagram of impedance control is shown in Fig. 5.

### 3.2 Simulation of Impedance Control

Simulation of impedance control shown in Fig. 5 is performed. Here, we use P-controller as a velocity controller. Simulation conditions are given below. External force  $F_h$  is put as a step signal.

Simulation result is shown in Fig. 6. It is indicated that by lightening virtual mass and virtual damper, push cart moves faster, in condition of same pushing force.

Table 3. Simulation conditions

|       | Without Control | With Control |
|-------|-----------------|--------------|
| $F_h$ | 50 N            | 50 N         |
| $M_i$ | No control      | 10 kg        |
| $B_i$ | No control      | 100 N/(m/s)  |

### 3.3 Experiment of Impedance Control

Experiment of impedance control shown in Fig. 5 is conducted. Here, steel plate with mass of 10 kg is used as a load. Other experimental conditions are given below.

Experimental results are shown in Fig. 7. It can be seen that with impedance control, the push cart robot moved faster while the pushing force is weaker.

Table 4. Experimental conditions

|                 | Case 1       | Case 2       |
|-----------------|--------------|--------------|
| Actual Mass $M$ | 40.6 kg      | 40.6 kg      |
| $F_h$           | Push by hand | Push by hand |
| $M_i$           | No control   | 10 kg        |
| $B_i$           | No control   | 100 N/(m/s)  |

### 3.4 Result Analysis of Impedance Control

For further analysis, we estimated mass and damper felt by the pusher, defined by  $M_f$  and  $B_f$ , using recursive least-squares (RLS) algorithm<sup>(14)</sup>. Here, pushing force  $F_h$ , cart velocity  $V$  and cart acceleration  $a_a$  of the time  $t$  is presented by  $F(t)$ ,  $V(t)$  and  $a_a(t)$  in form of column vector. Using  $x_i(t) = [a_a \ V]$ , covariance matrix  $\Gamma(t)$  and forgetting factor  $\lambda$ ,  $\theta(t) = [M_f(t) \ B_f(t)]$  is estimated by equation below.

$$\Gamma(t) = \frac{1}{\lambda} \left( \Gamma(t-1) - \frac{\Gamma(t-1) * x_i^t(t) * x_i(t) * \Gamma(t-1)}{\lambda + x_i(t) * \Gamma(t-1) * x_i^t(t)} \right) \quad (1)$$

$$\theta(t) = \theta(t-1) + \frac{\Gamma(t-1) * x_i^t(t) * \{F(t) - x_i(t) * \theta(t-1)\}}{\lambda + x_i(t) * \Gamma(t-1) * x_i^t(t)} \quad (2)$$

Using initial value  $\Gamma(t) = 1e + 6$  and  $\lambda = 0.995$ ,  $M_f(t)$  and  $B_f(t)$  derived by (1) with  $M_i = 10$  and  $B_i = 100$  is shown in Fig. 8. It can be seen that value of  $M_f(t)$  and  $B_f(t)$  is getting close to set  $M_i$  and  $B_i$ , being updated by the RLS.

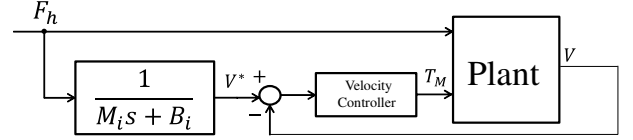


Fig. 5. Block diagram of impedance control

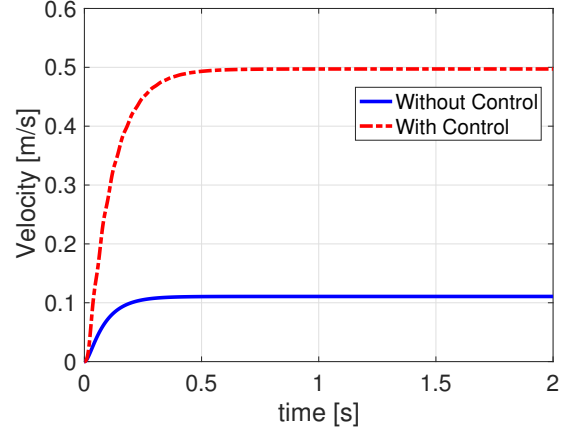


Fig. 6. Simulation result of impedance control

## 4. Friction Force Observer to Prevent the Slip of the Load

Impedance control enabled the robot to move with smaller pushing force. However, this may cause the slip of the load on the push cart robot, and end up with dropping the load. Goal of the push cart robot is to carry the load to the desired place, and it is necessary to prevent the load from slipping and dropping.

Model of the push cart robot with load is discussed, and then friction force observer is proposed to prevent the slip of the load.

### 4.1 Modeling of Friction

When there is a load on the push cart, the push cart take not only pushing force and driving force but also the friction force between the cart and the load. Model of the push cart robot is depicted in Fig. 9, with the friction force considered.

$f$  is the friction force exerted by the load.  $f$  is expressed by below, while  $\mu_s$ ,  $\mu_k$ ,  $m_b$  and  $a_b$  are coefficient of static friction, kinetic friction, mass and acceleration of load, respectively.

$$f = \begin{cases} m_b a_b & (m_b a_b \leq \mu_s m_b g) \\ \mu_k m_b g & (m_b a_b > \mu_s m_b g) \end{cases} \dots \dots \dots (3)$$

Here,  $\mu_s m_b g$  is the maximum static friction. In case of  $f = \mu_k m_b g$ , kinetic friction is working and the load on the push cart is slipping<sup>(15)</sup>. Friction force observer is proposed to observe the friction force and to prevent the load from slipping.

### 4.2 Friction Force Observer

When the friction force  $f$  exceeded maximum static friction  $\mu_s m_b g$  and turned into  $\mu_k m_b g$ , the load can be defined as slipping. Thus, the friction force must not exceed the maximum static friction to prevent the slip of the load. Practically,

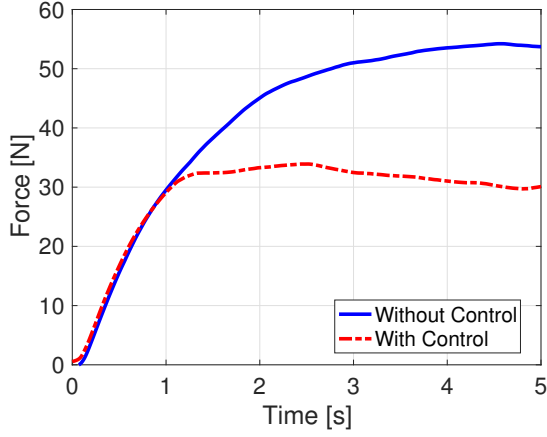
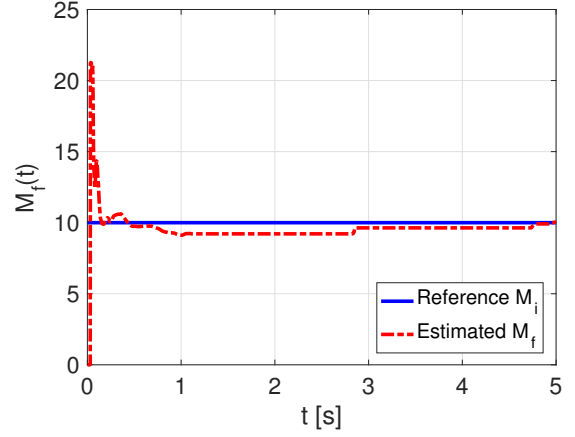
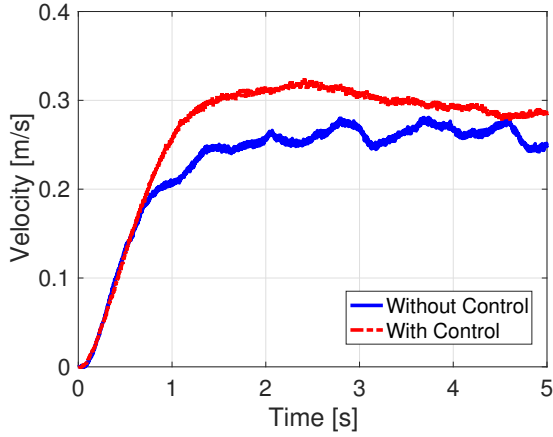
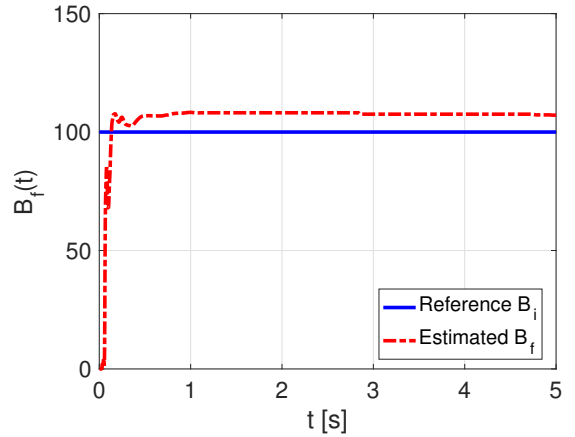
(a) External force  $F_h$ (a) Mass felt by the pusher  $M_f$ (b) Push cart velocity  $V$ (b) Damper felt by the pusher  $B_f$ 

Fig. 7. Experiment of impedance control

Fig. 8. Mass and damper felt by pusher estimated by RLS

$\mu_s$ ,  $\mu_k$  and even  $m_b$  may be unknown, so the friction force  $f$  should be estimated without the information of these parameters.

Here, we assume that only the pushing force  $F_h$ , the driving force  $F_d$ , and the friction force  $f$  work to the push cart robot. The equation of motion of push cart robot is given as follows;

$$m_a a_a = F_h + 2F_d - f, \quad (4)$$

where  $a_a$  is acceleration of push cart robot. Filtering (4) by LPF with cutoff frequency of  $f_c$ , estimated friction force  $\hat{f}$  is derived by

$$\hat{f} = \frac{2\pi f_c}{s + 2\pi f_c} (F_h + 2\hat{F}_d - m_a a_a). \quad (5)$$

For  $F_d$  used in (5), estimated driving force  $\hat{F}_d$  derived by the driving force observer shown below is used<sup>(16)</sup>.

$$\hat{F}_d = \frac{1}{r} \{T_s - (J_W s + B_W)\omega_W\} \quad (6)$$

Block diagram of the proposed friction force observer is shown in Fig. 10. Wheel angular velocity  $\omega_W$  and torsion

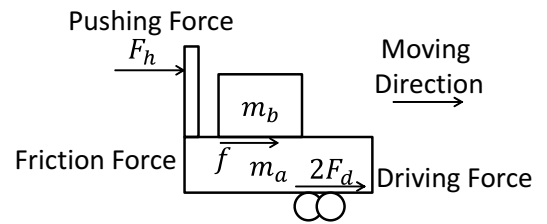


Fig. 9. Model of push cart robot and friction

torque  $T_s$  uses value measured by wheel side encoder and torque sensor, which are part of main characteristics of this push cart robot.  $a_a$  is derived by differentiating push cart speed  $V$ , measured by encoder in rear wheel.

### 4.3 Simulation of Friction Force Observer

#### 4.3.1 Estimating the Friction Force

In this simulation, ramp signal of 50 N is used as  $F_h$  and impedance control of  $M_i = 10$  kg,  $B_i = 0$  N/(m/s) is applied. Other simulation conditions are listed below.

Simulation result is shown in Fig. 11(a). The friction ob-

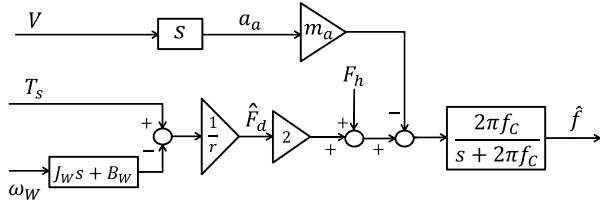


Fig. 10. Block diagram of friction force observer

served by the proposed observer precisely follows the actual friction. It is clearly observed that the friction has switched from static friction to kinetic friction at  $t = 1.2$  s.

From this result, it is indicated that the value of the friction force changes discontinuously in the switch between static friction and kinetic friction, causing the slip of the load. Differential of the estimated friction force is shown in Fig. 11(b), used in the next section to detect the slip.

Table 5. Simulation conditions

| Parameter                    |         | Value |
|------------------------------|---------|-------|
| Load mass                    | $m_b$   | 10 kg |
| Static friction coefficient  | $\mu_s$ | 0.2   |
| Kinetic friction coefficient | $\mu_k$ | 0.1   |
| Cutoff frequency of the LPF  | $f_c$   | 20 Hz |

#### 4.3.2 Preventing the slip of the load using Friction Force Observer

In this simulation, slip of the load is prevented using friction force observer. When the friction differential shown in Fig. 11(b) fell below the threshold  $-500$ , acceleration of the push cart is saved. That acceleration is used as the acceleration limit in the velocity control to prevent the slip. Other simulation conditions are same as before.

First, acceleration of the cart and the load without the acceleration limit is shown in Fig. 12(a). Cart acceleration  $a_a$  and load acceleration  $a_b$  differ after  $t = 1.2$  s, indicating the slip of the load.

Then, acceleration of the cart and the load with the acceleration limit using friction force observer is shown in Fig. 12(b).  $a_a$  and  $a_b$  coincides, showing that slip is prevented.

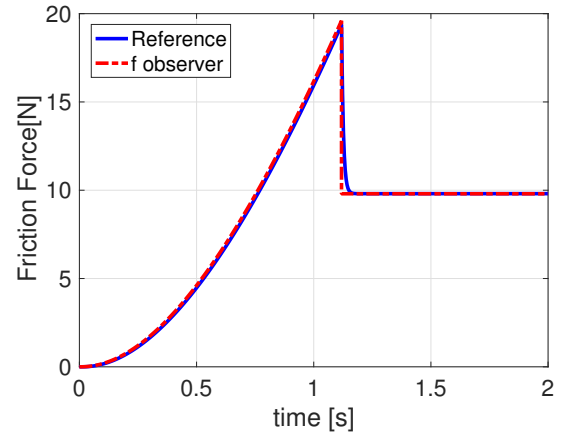
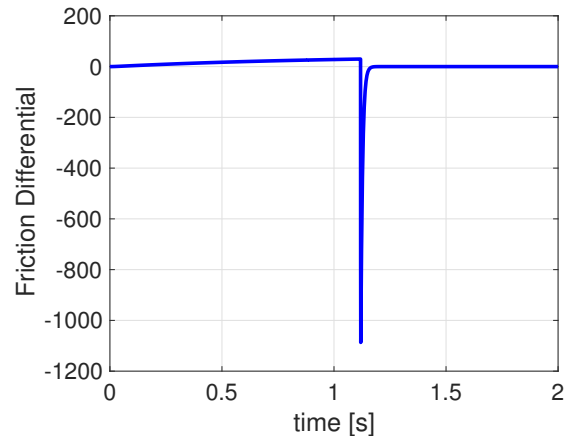
#### 4.4 Experiment of Friction Force Observer

Steel plate with mass of 10 kg is used as the load, and the push cart is moved by velocity control, instead of pushing it by hand. To make the load slippery, same steel plate is fixed on the cart as a foundation and the load is put on the plate. Case with the load slipping and load not slipping is compared, differed by reference signal of the motor angular velocity, as shown in Fig. 13. Other experimental conditions are listed below.

Experiment result is shown in Fig. 14. Positive peak is seen at  $t = 0.3$  s which might represent the slip, but there are several noises and disturbance in this experiment, so further improvement is needed.

### 5. Conclusion

We discussed the impedance control to push the push cart robot by smaller force, and proposed the friction force observer to prevent the load from slipping. Simulation showed effectiveness of both the impedance control and the friction

(a) Friction force  $f$  and estimated friction force  $\hat{f}$ 

(b) Differential of the estimated friction force

Fig. 11. Simulation of friction force observer

Table 6. Experimental conditions

|                             | No Slip | With Slip |
|-----------------------------|---------|-----------|
| $m_a$                       | 40.6 kg | 40.6 kg   |
| $m_b$                       | 10 kg   | 10 kg     |
| Gradient of $\omega_{Mref}$ | 600     | 700       |

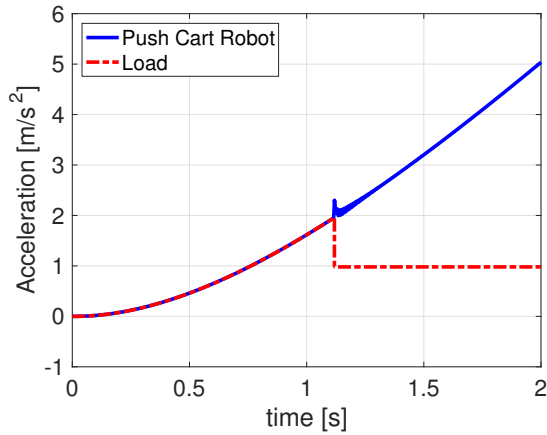
force observer, while experiment of the friction force observer had problems.

Impedance control has room for further research, such as to realize stable run even on slopes and hills, or to detect the contact other than the user to prevent accident during the use.

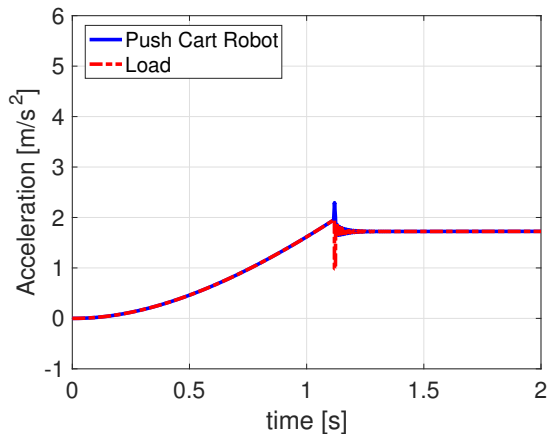
The friction force observer needs improvement to observe friction more exactly, and to actually use the data of friction to prevent the slip. Further consideration of velocity reference could be made, to realize faster transportation of the load, and more comfortable use for user.

### References

- (1) M. Homayounzade, "Adaptive Position / Force Control of Robot Manipulators with Force Estimation", RSI/ISM International Conference on Robotics



(a) Acceleration of the cart and the load without acceleration limit



(b) Acceleration of the cart and the load with acceleration limit by friction force observer

Fig. 12. Simulation of slip prevent using friction force observer

- and Mechatronics, pp. 736–741, 2014
- (2) S. Sakaino, K. Ohnishi, "An approach for force control of redundant robots under unknown environment", IEEE International Symposium on Industrial Electronics, pp. 1312–1317, 2008
  - (3) L. Lu, J. Wen, "Human-Directed Robot Motion / Force Control for Contact Tasks in Unstructured Environments", 2015 IEEE International Conference on Automation Science and Engineering (CASE), pp. 1165–1170, 2015
  - (4) Y. Kawai, Y. Yokokura, K. Ohishi, "High Back-drivable Pseudo I-PD Torque Control Using Load-side Torque Observer With Torsion Torque Sensor", IEEE Advanced Motion Control, Auckland New Zealand, pp. 175–180, 2016
  - (5) P. Weiss, P. Zenker and E. Maehle, "Feed-forward friction and inertia compensation for improving backdrivability of motors," 2012 12th International Conference on Control Automation Robotics & Vision (ICARCV), Guangzhou, pp. 288–293, 2012
  - (6) T. Yamashita, T. Mashimo, N. Takesue and K. Terashima, "Safeness of a robot arm using ultrasonic motors with high responsiveness and backdrivability," System Integration (SII), 2014 IEEE/SICE International Symposium on System Integration, Tokyo, pp. 28–33, 2014
  - (7) T. Hayashi, F. Matsukawa and S. Jeong, "Power-assist transportation based on virtual impedance control for self-balancing robotic cart," 2013 13th International Conference on Control, Automation and Systems (ICCAS 2013), Gwangju, 2013, pp. 1068–1072.
  - (8) M. Ruderman, W. Maebashi, M. Iwasaki, "Semi-dual Loop Control of Two-Mass Actuator System using Luenberger State Observer", Industrial Electronics Society, IECON 2013 - 39th Annual Conference of the IEEE, pp.

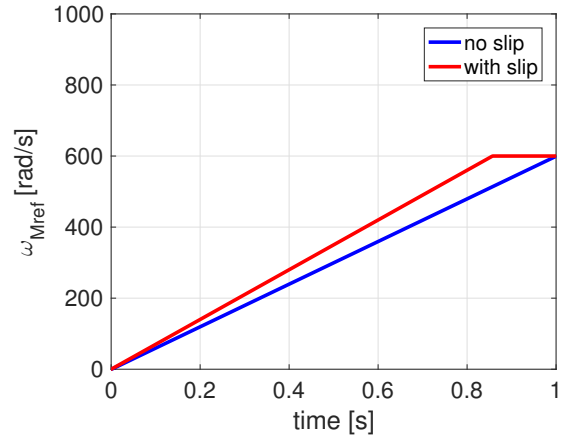
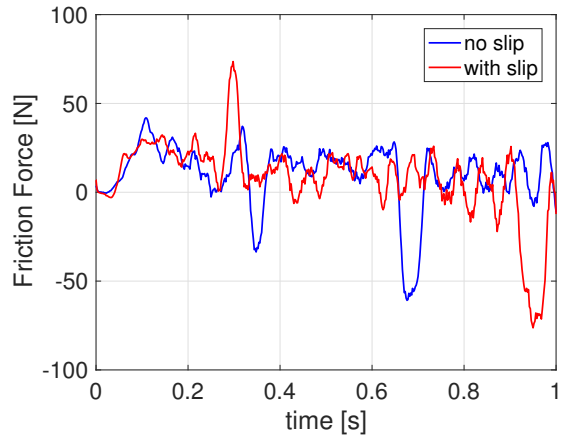

 Fig. 13. Motor angular velocity reference  $\omega_{Mref}$  used in the experiment


Fig. 14. Observed friction force in the experiment

- (9) B. Zeng, R. Ding, Z. Zhou, Z. Wang and H. Xu, "Parameter optimization of harmonic gear drive based on hybrid genetic algorithm," 2012 International Conference on Quality, Reliability, Risk, Maintenance, and Safety Engineering, Chengdu, pp. 1089–1092, 2012
- (10) S. Yamada, K. Inukai, H. Fujimoto, K. Omata, Y. Takeda, S. Makinouchi, "Joint torque control for two-inertia system with encoders on drive and load sides", IEEE 2015, pp. 396 – 401, 2015
- (11) Y. Yokokura, K. Ohishi, K. Saito, A. Shimamoto and Y. Yamamoto, "Verification of load-side acceleration control for a 2-inertia resonant system with a torsion torque sensor," 2015 IEEE/SICE International Symposium on System Integration (SII), Nagoya, pp. 271–276, 2015
- (12) M. Yamashita, T. Soeda, "Anti-slip re-adhesion control method for increasing the tractive force of locomotives through the early detection of wheel slip convergence", EPE'15 ECCE-Europe, 2015
- (13) J. Li, L. Liu, Y. Wang and W. Liang, "Adaptive hybrid impedance control of robot manipulators with robustness against environment's uncertainties," 2015 IEEE International Conference on Mechatronics and Automation (ICMA), Beijing, pp. 1846–1851, 2015
- (14) H. Fujimoto and Bin Yao, "Multirate adaptive robust control for discrete-time non-minimum phase systems and application to linear motors," in IEEE/ASME Transactions on Mechatronics, vol. 10, no. 4, pp. 371–377, 2005
- (15) K. Tadokoro, Y. Konishi, N. Araki and H. Ishigaki, "Positioning Control of a 2-Mass Spring System with Static and Kinetic Friction Using Hybrid Controller," 2008 3rd International Conference on Innovative Computing Information and Control, Dalian, Liaoning, pp. 197–197, 2008
- (16) J. Amada, H. Fujimoto, "Torque Based Direct Driving Force Control Method with Driving Stiffness Estimation for Electric Vehicle with In-Wheel Motor", IECON 2012 - 38th Annual Conference on IEEE Industrial Electronics Society, pp. 490–4909, 2012